Different nitrosative-induced microtubular modifications and testosterone neuroprotective effects on high-D-glucose-exposed neuroblastoma and glioma cells

Sergio Gadau, Gianluca Lepore, Marco Zedda, Arcadia Mura, Vittorio Farina

Department of Animal Biology, University of Sassari, Italy.

Correspondence to:	Dr. Sergio Gadau
	Department of Animal Biology, University of Sassari, Via Vienna 2, Italy.
	PHONE: +39 079229596; FAX : +39 079229432; E-MAIL: sgadau@uniss.it

Abstract

OBJECTIVES: Diabetic complications can often affect the central nervous system since the chronic exposure to hyperglycemia can result in the production of high concentration of reactive oxygen species with subsequent damage of several cell structures such as the cytoskeleton. In order to antagonize the oxidative status many substances have been tested as antioxidants. In the present work attention has been focused on the possible nitrosative effect of hyperglycemia on microtubular network of neuroblastoma and glioma mortalized cell lines, testing the possible neuroprotective effect of testosterone.

METHODS: Neuroblastoma (C1300) and glioma (C6) cell lines were cultured in the presence of 300mM (C1300) or 310mM (C6) D-glucose, with or without 50nM testosterone. After 72hrs, morphology, growth rate, cell viability and catalase activity were evaluated. In addition, with the aim to detect any changes in the amount of tubulin isoforms, Western blot analysis was performed.

RESULTS: In D-glucose-exposed cells, it was found a down-regulation of tubulin isoforms and an increase in 3-nitro-L-tyrosine and subsequent modifications in cell morphology, growth rate, viability and catalase activity. All these changes were more severe in neuroblastoma than in glioma cell line. When testosterone was added to the medium, all the parameters were very similar to controls. This neuroprotective action was well-detectable in C1300 cells, whereas testosterone was not able to recover significantly in C6 cells.

CONCLUSION: Our results displayed: i) a selective action of high glucose on microtubules; ii) a different sensitivity to oxidative stress in neuronal and glial cells; iii) a different neuroprotective action of testosterone on neuronal and glial cells.

INTRODUCTION

Oxidative stress is a condition where there is an imbalance between generation and elimination of reactive oxygen species (ROS) and reactive nitrogen species (RNS) such as nitric oxide, peroxynitrite, and hydroxyl radicals and it has been associated with a wide range of pathological conditions. It is known that all aerobic organisms suffer oxidative damage since ROS and RNS are produced during mitochondrial respiration (Chance *et al.* 1979; Halliwell, 1992; Halliwell, 2001; Halliwell, 2006). Cells are usually provided with a variety of endogenous protective systems

ORIGINAL ARTICLE

(e.g. catalase, glutathione, superoxide dismutase, etc.) to counterbalance the potentially dangerous ROS and RNS. In case these defense mechanisms are inadequate, the cell will become dysfunctional or die. The central nervous system is particularly vulnerable to oxidative insults because of the high rate of O_2 utilization, the high amount of easily peroxidizable fatty acids and relatively poor concentration of antioxidant defence systems (Andersen, 2004; Emerit *et al.* 2004; Sayre *et al.* 2008).

Recently, a considerable amount of evidence has pointed out the existence and the critical role of reciprocal interactions between glial and neuronal cells. Astrocytes appear intimately associated with the synapse, enwrapping both presynaptic and postsynaptic terminals. This close relationship provides many functional interactions between astrocytes and neurons. Indeed, though neurons are considered more metabolically active than glial cells, the latter seem to be involved in the organization of a proper environment for the neuronal functioning (Kurosinski and Gotz, 2002). Although with different susceptibility, both neurons and glial cells are continuously exposed to ROS or RNS, leading to excitotoxicity and apoptosis. These processes may play a role in the pathogenesis of the so-called glianeuronal disease (Hollensworth *et al.* 2000; Khanna and Nehru, 2007). Indeed, under oxidative stress conditions, neuronal cell death is always accompanied by astroglial cell hypertrophy, cytoskeletal changes and production of cytotoxic molecules (Acarin *et al.* 2005).

Various mechanisms are supposed to be at the basis of the formation of ROS and RNS. Glucose oxidation is known to be a considerable source of free radicals mainly when the normally efficient metabolism of glucose is altered with subsequent overloaded metabolic pathways (Maritim *et al.* 2003; Allen *et al.* 2005). It is well-known that D-glucose is an essential substrate for the brain whose activity depends on the availability of this hexose. Physiologically, both neurons and astrocytes have high rates of glucose utilization, largely through oxidative metabolism, as its primary fuel for energy generation (Guillod-Maximin *et al.* 2004; McCall, 2004; Hertz and Kala, 2007).

The hyperglycemic condition can be considered a potent initiator of apoptosis (Delaney *et al.* 2001) through the excessive production of ROS with formation of peroxynitrite and subsequent damage of cellular proteins, membrane lipids, nucleic acids and eventually cell death. One of the early events in cell injury caused by oxidative stress is considered the impairment of cytoskeletal structures. Indeed, peroxynitrite can react with tyrosine to produce 3-nitro-L-tyrosine. Accumulation of 3-nitro-L-tyrosine has been reported in several tissues of diabetic mice, rats and humans (Thuraisingham *et al.* 2000; Pacher *et al.* 2005; Drel *et al.* 2006). Moreover, increased 3-nitro-L-tyrosine immunoreactivity has been demonstrated in peripheral nervous system (Cheng and Zochodne, 2003) during experi-

mental diabetic conditions. This end product, considered a footprint for peroxynitrite mediated damage, can impair cellular structures such as microtubules, with an irreversible block of their characteristic dynamics (Eiserich *et al.* 1999; Chang *et al.* 2002). In the last years, experimental studies dressed to recognize new approach against oxidative stress have been indicated several substances as neuroprotective. Among these, sexual hormones exhibit neuroprotective and neurotherapeutic effects on CNS and PNS. In particular, testosterone, like other androgens, may exert biological effects on neural cells, leading to changes in cell shape, survival and regeneration (Ahlbom *et al.* 2001; Hammond *et al.* 2001; Pike, 2001; Coers *et al.* 2002; Tanzer and Jones, 2004; Túnez *et al.* 2007).

As the role of nitrosative component of oxidant-induced injury during hyperglycemic conditions has not been well-understood, aim of the present work is to evaluate the pattern of sensitivity of two different cell lines, C1300 neuroblastoma and C6 glioma cells, under high-D-glucose exposure. The possible oxidative effects on the microtubular network have been monitored in the presence or not of the neurotrophic testosterone. Our attention has been paid on cytoskeleton as in a previous work of ours we found a selective incorporation of 3-nitro-L-tyrosine into α-tubulin in a neuroblastoma cell line exposed to high concentration of D-glucose (Gadau *et al.* 2008).

MATERIALS AND METHODS

For all experimental procedures, undifferentiated C1300 mouse neuroblastoma cells and C6 rat glioma cells (American Type Culture Collection, Rockville, MD, USA) were seeded at a concentration of 5.6×10^5 per ml and grown in phenol-red-free RPMI-1640 medium supplemented with 10% heat-inactivated dextran-coated charcoal-stripped newborn calf serum, 2 mM L-glutamine, 100 units/ml penicillin G and 100 µg/ml streptomycin sulfate. Cells were incubated for 72 hours at 37°C in a 5% CO_2 humidified atmosphere according to the following protocols:

i) C1300 with standard medium (Ctrl cells);

ii) C1300 with 110mM D-glucose (G cells);

iii) C1300 with 110mM D-glucose and 50 nM testosterone (G+T cells);

iv) C6 with standard medium (Ctrl cells);

v) C6 with 300mM D-glucose (G cells);

vi) C6 with 300mM D-glucose and 50 nM testosterone (G+T cells).

As regards the D-glucose dose employed, a dose-response curve was performed for both cell lines (data not shown). In C1300 cells the first morphological signs of suffering were appreciable at 110mM D-glucose. In contrast, in C6 cells at the dose of 110mM there was a normal growth without any morphological alteration. A concentration of 300mM D-glucose was the lowest dose displaying evidence of C6 cell suffering. Hence,

the results and pictures related to C6 cells presented in this paper deal with 300mM D-glucose.

Testosterone was dissolved in absolute ethanol and then diluted in basal medium to the final concentration. In order to estimate the morphological features, monolayers were observed in the living state under phase-contrast optics and photographed. To check the possible toxic effects of ethanol, a further control was performed incubating cells for 72hrs in medium containing absolute ethanol at the same concentration used to dissolve testosterone (0.0001% v/v).

Cells cultured as above were rinsed with PBS and suspended in microtubule stabilizing solution (5mM TRIS HCl, 2mM EGTA, 0.1mM phenyl-methyl-sulfonyl fluoride, pH 8.0) supplemented with protease inhibitors (Complete-mini, Roche, Basel, Switzerland). The lysate was centrifuged at 15,000 rpm for 15 min. Protein content was determined (DC Protein Assay, BioRad, CA, USA) and equal amounts of proteins (40 µg) were separated on 10% SDS polyacrylamide gel with Mini PROTEAN Tetra Cell (BioRad) and then transferred onto 0.45 mm nitrocellulose membranes with Trans-blot semi-dry (BioRad). Blots were blocked for 2 hrs at room temperature with 5% (w/v) non-fat dried milk in Tris-buffered saline Tween 20. After soaking for 3hrs, membranes were incubated overnight at 4°C with antibodies against tyrosinated α-tubulin (monoclonal, clone TUB-1A2, Sigma, 1:1,000), acetylated α-tubulin (monoclonal, clone 6-11B-1, Sigma, 1:1,000), total α-tubulin (monoclonal, clone DM1A, Sigma, 1:1,000), actin (monoclonal, clone AC-40, Sigma, 1:1,000), 3-nitro-L-tyrosine (polyclonal, Sigma, 1:500) and androgen receptor (polyclonal, Sigma, 1:100). Blots were then incubated with the corresponding anti-mouse or anti-rabbit IgG alkaline phosphatase-conjugated antibody (Sigma) for 1 hr at 37°C at 1:1,000 or 1:30,000 dilution respectively. Blots were subsequently detected by incubating the membranes with nitro blue tetrazolium/5bromo-4-chloro-3-indolyl phosphate (NBT/BCIP, Roche) and heat fixed. Optical density of the bands was evaluated using the freeware Scion Image software.

C1300 and C6 cells treated following the protocols above indicated underwent proliferation assay using a 96-well microtiter plates. At the end of each treatment, the medium was removed and the wells were washed with PBS. The 3-(4,5-dimethylthiazol-2-yl)-2,5-diphenyltetrazolium bromide (MTT) assay was performed by adding 20µl MTS (5 mg/ml, MTT, Cell Titer 96, Promega, Madison, WI, USA). The plate was mixed with the microplate shaker for 5 minutes to make sure that all purple crystals were dissolved and then incubated for 1hr at 37°C. MTS was reduced by living cells into a coloured formazan compound that is soluble in tissue culture medium. Absorbance was measured setting the automatic microtiter reader at 492 nm (Uniskan II, Labsystem, Helsinki, Finland), in the presence of an appropriate blank (without cells). The blank

reading was subtracted from experimental readings, and cell viability was expressed as the percentage of the absorbance values of SD-treated groups to untreated controls.

Cell viability was determined by a double-staining procedure using bis-benzimide (Hoechst 33342, Sigma) and propidium iodide (PI, Sigma). Cells positively stained with PI were considered to be dead. Dead and surviving C1300 and C6 cells were counted from photomicrographs and cell death rate was evaluated as dead cells vs total cell number × 100. Intra-observer and inter-observer variability was each < 2%.

Catalase activity was estimated according to the method of Aebi (1984). Catalase degrades hydrogen peroxide which is measured directly by the decrease in the absorbance at 240 nm (Uniskan II). Ice-cold cells were collected and sonicated to rupture cell membranes. The hydrogen peroxide was diluted with PBS, pH 7.0 and its initial absorbance was adjusted between 0.5 and 0.6 of absorbance unit. Catalase activity was expressed as U/ml.

Average values used for analysis are representative of five experiments for each protocol. Data are expressed as mean ± standard error (SEM), and the inter-group analysis was done by Student's *t*-test or ANOVA. Statistical significance was accepted when $p < 0.05$.

RESULTS

Cell morphology and proliferation assay

C1300 cells. After 72 hrs of culture, when observed under phase contrast optics, cells treated with 110mM D-glucose displayed a reduced number and several morphological alterations, such as globular shape, vacuols and lack of cytoplasmic processes in comparison with Ctrl cells. In the presence of testosterone recovery of all morphological features was appreciable. This tendency was confirmed by the proliferation assay. Significantly, in D-glucose-exposed cells (G cells) MTS bioreduction revealed a decrease in proliferation rate to approximately 70% of Ctrl cells. When testosterone was added to the medium (G+T cells), the proliferation rate became similar to Ctrl cells (***Fig. 1***).

C6 cells. After exposure to 300mM D-glucose, the morphological alterations were less detectable than in C1300 cells. Indeed, after 72 hr-exposure, cells still displayed their typical oval shape and a lot of cytoplasmic processes. Even after testosterone administration (G+T cells) cell shape remained unchanged. As regard the number of the cells, G cells decreased their number of about 40% in comparison with Ctrl. Testosterone exposure (G+T cells) was followed by a moderate recovery in cell growth of about 20% in comparison with G cells, although the confluent state was not reached (***Fig. 2***).

Viability assay

The possible deleterious effect of high-glucose exposure and the neuroprotective effects of testosterone were

Sergio Gadau, Gianluca Lepore, Marco Zedda, Arcadia Mura, Vittorio Farina
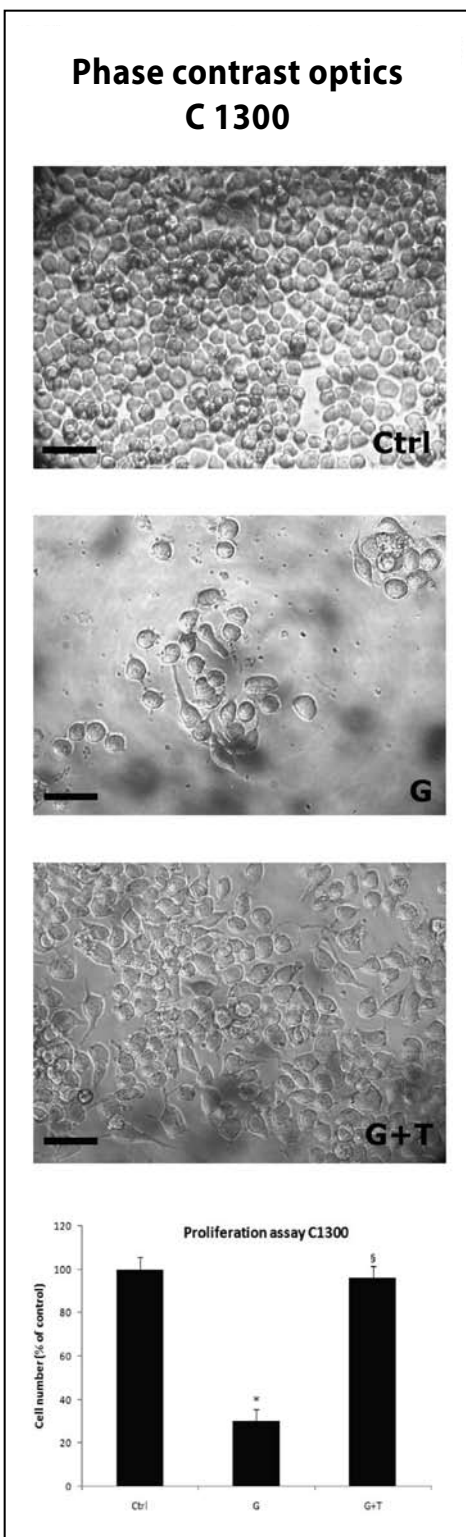
Fig. 1. Phase contrast optics and proliferation assay C1300. 110mM D-glucose-exposed cells (G cells) display several morphological alterations. In the presence of testosterone (G+T cells) monolayers exhibit morphological features similar to Ctrl. Bar =30µm. The diagram of proliferation shows a severe inhibition of growth rate in D-glucose-exposed cells and a complete recovery in the presence of testosterone, where the values are similar to Ctrl. Data are shown as percentage of maximum value and expressed as mean ± SEM. Each column represents the average of six single experiments.
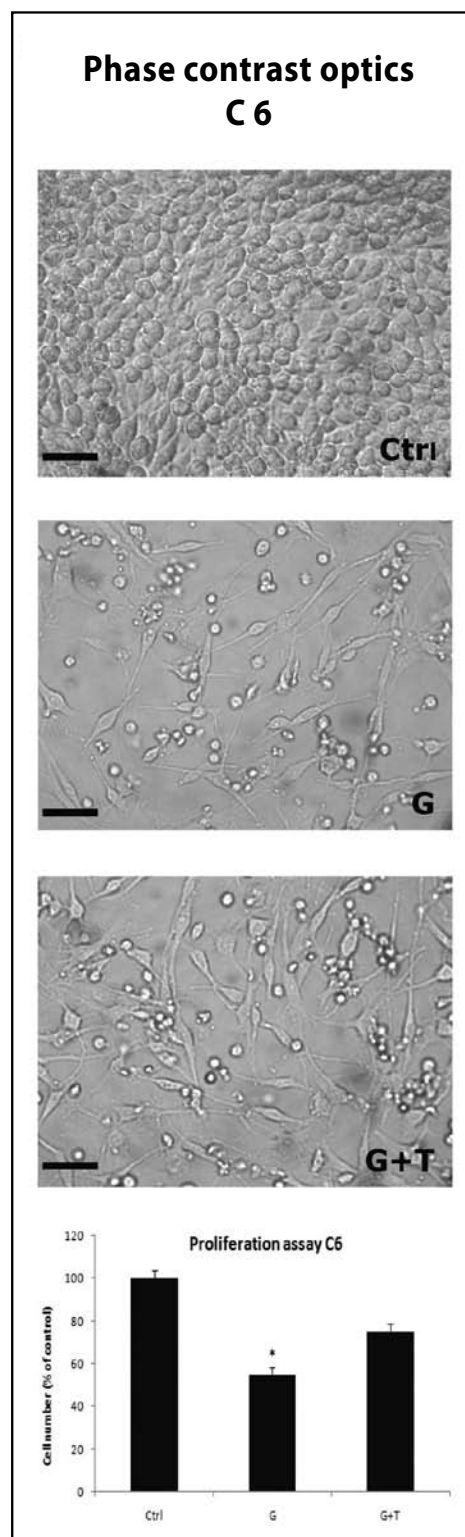* indicates significant differences from Ctrl (p < 0.05), § indicates significant differences from G cells.

Fig. 2. Phase contrast optics and proliferation assay C6. After 72hrs of 300mM D-glucose exposure, glial cells display severe morphological alterations. In the presence of testosterone (G+T cells), cells recover their morphology. Bar=25µm. The proliferation assay shows that growth rate declines in D-glucose cells (G cells). When testosterone is added to the medium (G+T cells), little improvement of proliferation rate is evident. Data are shown as percentage of maximum value and expressed as mean ± SEM. Each column represents the average of six single experiments.
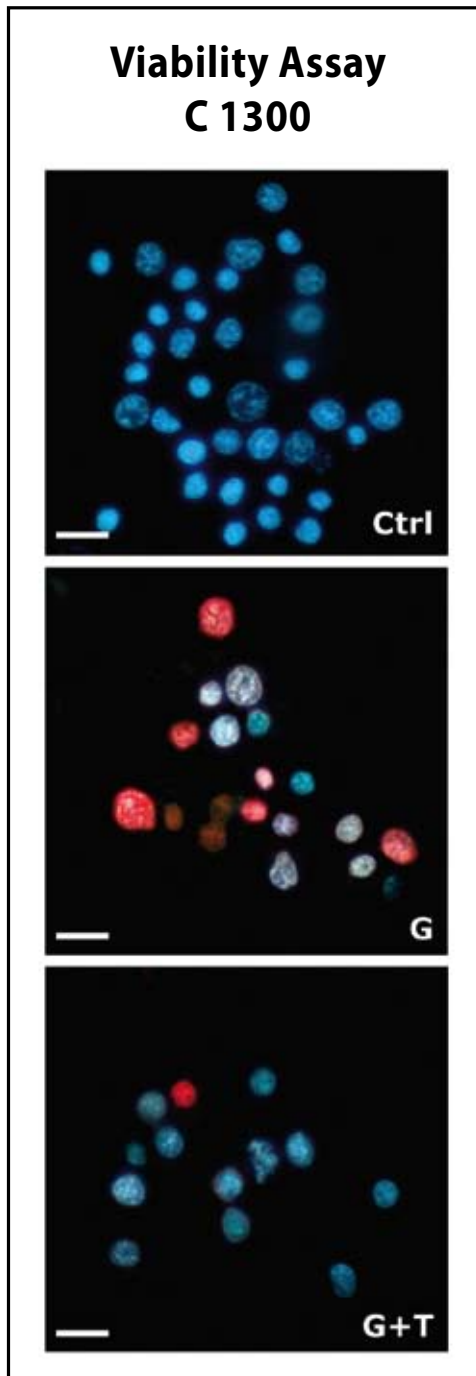* indicates significant differences from Ctrl (p < 0.05).

Fig. 3. Viability assay C1300. Hoechst 33342/PI staining reveals a high number of dead cells (red nuclei) in G cells. In contrast, a great deal of living cells (blue nuclei) are present in Ctrl and in G+T cells. Bar =15μm.

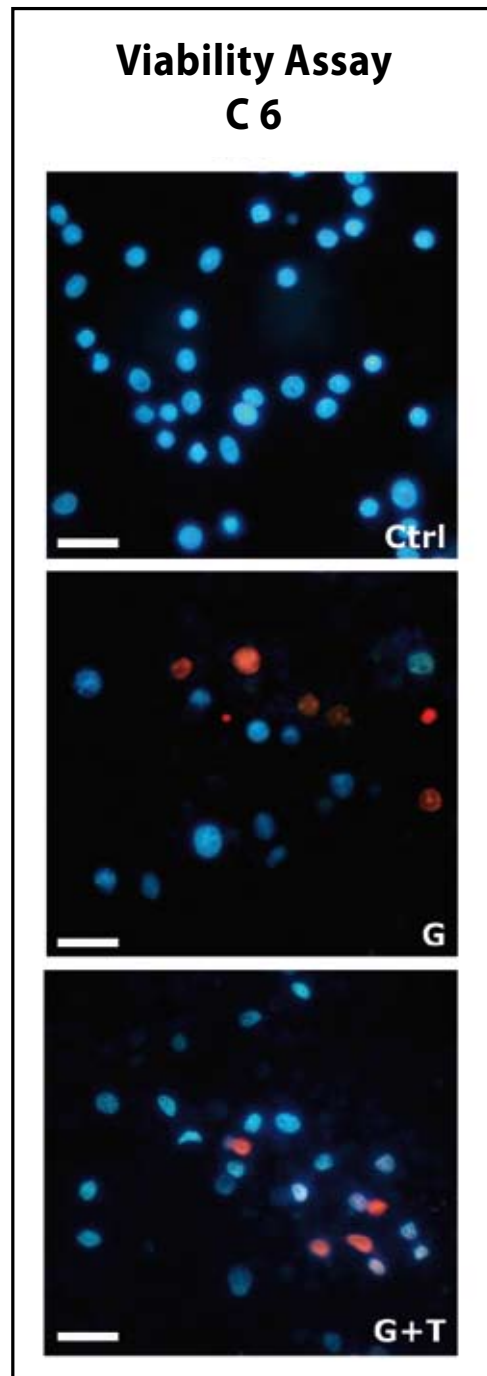**Fig. 4. Viability assay C6.** Hoechst 33342/PI staining reveals few dead cells (red nuclei) in G cells. In the presence of testosterone, the recovery of cell viability is not significant. Bar =15μm.

further studied using Hoechst 33342 and PI double staining. After 72hrs, C1300 Ctrl cells exhibited a high number of Hoechst-positive cells (more than 90%) with homogeneous and compact nuclear morphology. With the addition of 110mM D-glucose in C1300 (G cells) a mortality rate of about 85% (PI-positive) was recorded. Because PI is membrane impermeant and generally excluded from viable cells, PI-positive cells were dead cells. However, the exposure of cultured cells to 50nM testosterone (G+T cells) resulted in significant increase in viable cells (Hoechst-positive cells, average 80%). *Fig. 3.*

In C6 cells, Ctrl exhibited a high number of Hoechst-positive cells (more than 90%). D-glucose treatment showed a different trend in viability in comparison with C1300 cells. Indeed, C6 cells exposed to 300mM
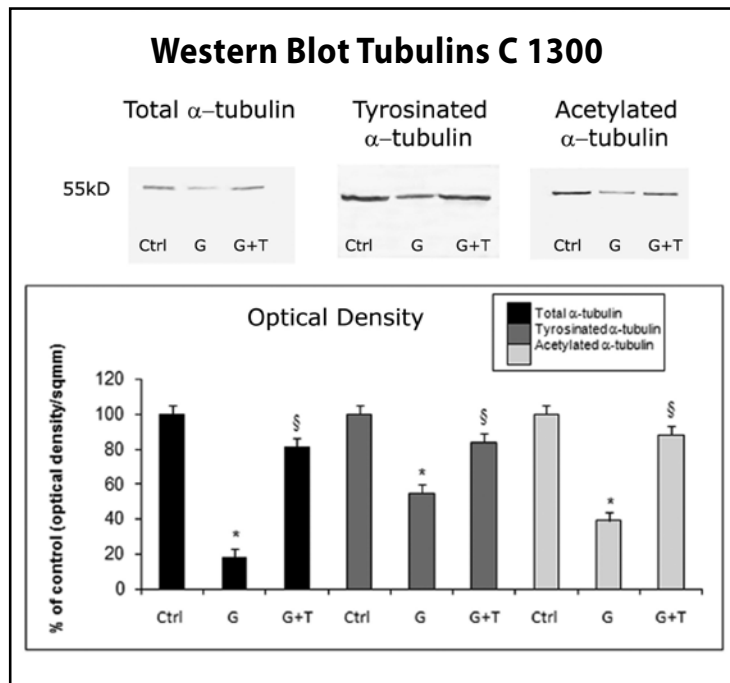
Western Blot Tubulins C 1300

Fig 5. Western blot tubulins C1300. Downregulation of α-tubulin isoforms in D-glucose-exposed cells (G cells) in comparison with Ctrl. Tubulin upregulation in response to testosterone (G+T cells) is well-appreciable with a pattern of expression of all tubulins very similar to Ctrl. Tubulin subunit is visualized as a single band migrating at approximately 55kD. The diagrams represent the optical density of the bands. * indicates significant differences from Ctrl (p < 0.05), § indicates significant differences from G cells.
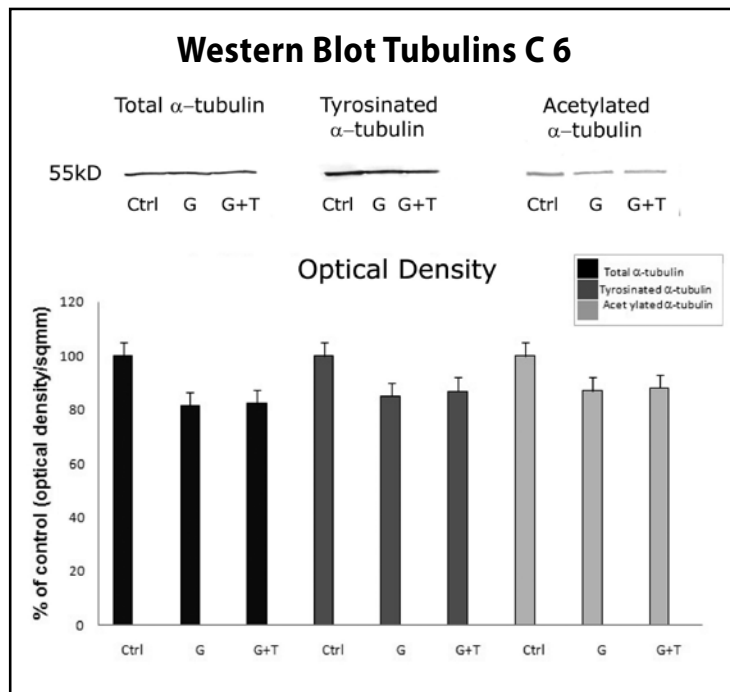
Western Blot Tubulins C 6

Fig 6. Western blot tubulins C6. Little downregulation of α-tubulin isoforms in D-glucose-exposed cells (G cells) with no significant differences from Ctrl and G+T cells. The diagrams represent the optical density of the bands.

D-glucose displayed few PI-positive cells. In the presence of testosterone, the recovery of cell viability was not significant with slightly lower PI-positive cell number in comparison with both G and Ctrl cells (**Fig. 4**).

Western blot analysis

Western blot analysis showed in C1300 D-glucose exposed cells (G cells) a downregulation of total α-tubulin, tyrosinated α-tubulin and acetylated α-tubulin in comparison with Ctrl cells. In contrast, cells exposed to testosterone (G+T cells) revealed a tubulin amount that was closer to Ctrl (**Fig. 5**). In C6 D-glucose cells (G cells) the decrease in tubulin expression was scarcely evident in comparison with Ctrl. No significant changes were detectable in the presence of testosterone (**Fig. 6**). Western blot analysis of another cytoskeletal component, actin, revealed any differences neither in C1300 nor C6 cells (**Fig. 7**).

The antibody against 3-nitro-L-tyrosine revealed in C1300 cells a higher amount of a single nitrated protein co-migrating with tubulin in cells exposed to glucose (G cells) in comparison with Ctrl cells. In the presence of testosterone, the amount of 3-nitro-L-tyrosine was low as in Ctrl. In C6 D-glucose-exposed cells, the amount of 3-nitro-L-tyrosine was high, and its decrease was not significant (**Fig. 8**) when testosterone was added (G+T cells). Western blot analysis was also performed on Ctrl cells in order to visualize possible different expression in androgen receptor between C1300 and C6 cells, and a higher amount of androgen receptor was ascertained in C1300 than C6 cells (**Fig. 9**). From all blots obtained, a diagram was drawn in order to quantify the optical density of the bands.

Catalase activity test

Catalase activity was checked in all the experimental conditions. Catalase activity significantly decreased in D-glucose-exposed C1300 cells as far as about 70% of Ctrl cells. In the presence of testosterone, the values of catalase activity came back to those observed in Ctrl cells. In C6 cells, the depletion in catalase activity produced by the administration of 300mM D-glucose was about 40% of Ctrl cells. Moreover, testosterone treatment (G+T cells) did not prevent significantly the D-glucose-induced catalase activity decrease in these cells (**Fig. 10**).
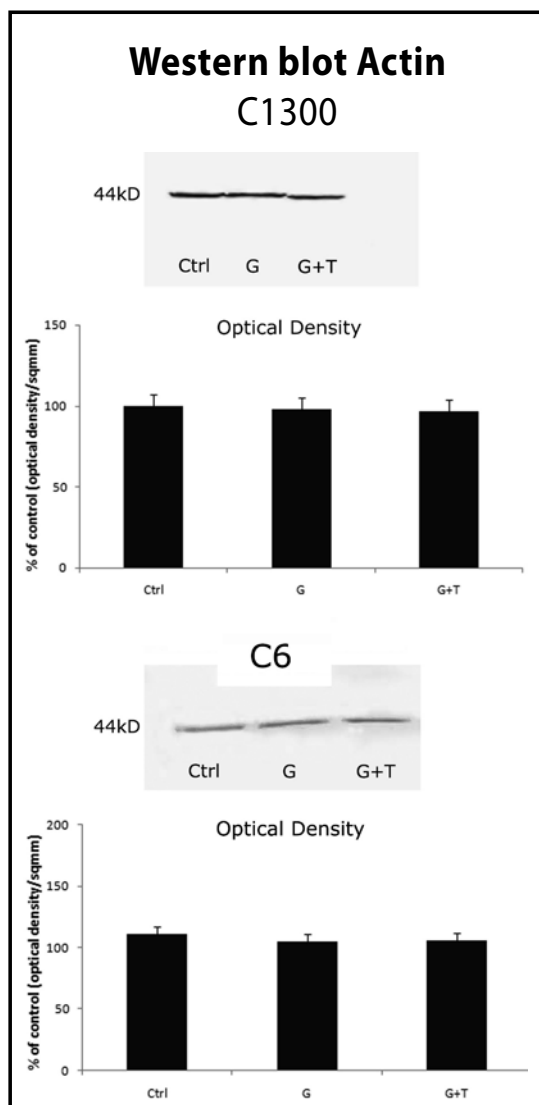
Fig 7. Pattern of actin expression in C1300 and C6 cells. No changes in actin expression are observed after each treatment in both cell lines. The diagrams represent the optical density of the bands.
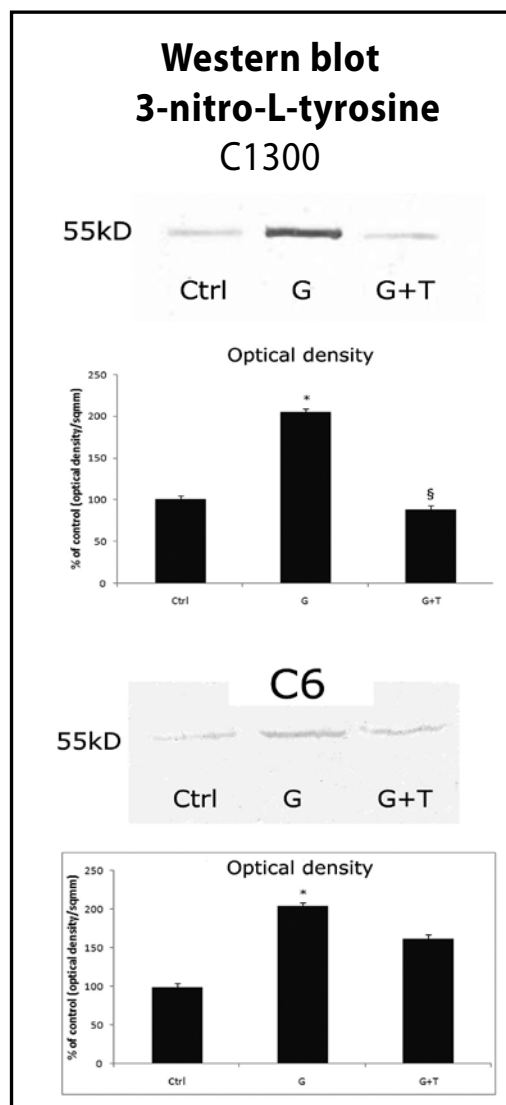

Fig 8. Pattern of 3-nitro-L-tyrosine in C1300 and C6 cells. In C1300 cells, the amount of 3-nitro-L-tyrosine is higher in G cells than in Ctrl. In the presence of testosterone (G+T cells), the level of 3-nitro-L-tyrosine is very similar to Ctrl. In contrast, in C6 cells the amount of 3-nitro-L-tyrosine is higher both in G and G+T cells than in Ctrl. The diagrams represent the optical density of the bands. * indicates significant differences from Ctrl (p < 0.05), § indicates significant differences from G cells.

DISCUSSION

The experimental results presented here underline two crucial points: i) D-glucose exposure impairs the microtubular network in both the cell lines studied: ii) testosterone anti-oxidant effects vary depending on the neuronal or glial origin of the cell line. The first significant result of our experiments seems to be a selective action of D-glucose on microtubular network. Indeed, in both neuroblastoma and glioma D-glucose-exposed cells a decreased amount in total α-tubulin, tyrosinated α-tubulin and acetylated α-tubulin was observed. This trend was more prominent in C1300 than C6 cells. D-glucose effects on tubulins in both cell lines could be related to the presence of 3-nitro-L-tyrosine. Western

blot analysis revealed a higher amount of 3-nitro-L-tyrosine, a useful biomarker of oxidative stress mediated by NO-derived oxidants, in D-glucose cells in comparison with Ctrl. Many data in the literature reported that 3-nitro-L-tyrosine can be selectively and irreversibly incorporated at the carboxyl terminus of α-tubulin (Eiserich *et al.* 1999; Chang *et al.* 2002; Phung *et al.* 2006), blocking the physiological dynamics of microtubules. It is well-known that microtubules are essential cytoskeletal components with a crucial role in many physiological cell activities such as cell division, motility, morphology, neurite extension and growth cone
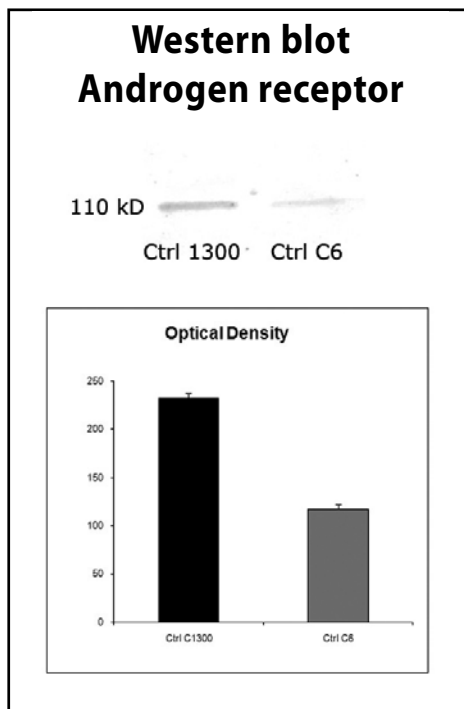
Fig 9. Western blot analysis of androgen receptor expression in C1300 and C6 controls. Higher amount of androgen receptor in C1300 cells than in C6 cells. The diagram represents the optical density of the bands.

Fig 10. Catalase activity assay. In C1300, impairment of catalase efficiency is more marked in D-glucose-exposed cells (G cells) than in Ctrl. In the presence of testosterone (G+T cells), the activity of catalase system becomes very similar to Ctrl. In C6, a decrease in catalase activity is well-detectable in the presence of high glucose. The administration of testosterone does not provoke any significant increase in catalase activity. * indicates significant differences from controls ($p < 0.05$), § indicates significant differences from G cells.

advancement, this last in cooperation with actin (Erck *et al.* 2005; Fukushima *et al.* 2009; Marcos *et al.* 2009).

The two cell lines employed in our work normally reach the confluent state in 48hrs, and during their growth they emit 2-4 cytoplasmic processes. Once reached the confluent state, cells lose their cytoplasmic elongations because of the cell-cell contact. The detrimental effect provoked by 3-nitro-L-tyrosine incorporation into tubulin may explain the alterations of cell morphology (globular shape and absence of cytoplasmic processes), growth rate (reduced number of cells), viability assay (high number of dead cells) observed in C1300 and C6 D-glucose-exposed cells. Our findings confirm those reported in the literature that underline how the impairment of microtubular dynamics caused by the irreversible incorporation of 3-nitro-L-tyrosine, is responsible for morphological alterations and apoptosis (Mihm *et al.* 2001; Peluffo *et al.* 2004; Zedda *et al.* 2004; Blanchard-Fillion *et al.* 2006). The idea that the main action of D-glucose was addressed to microtubules is strengthened by the examination of other cytoskeletal components such as microfilaments. Since there is a strict cooperation between microtubules and actin, mainly as regards slow axonal transport (Zhou *et al.* 2004), the expression of actin was evaluated. In the present study the unchanged expression of actin confirms the selective action of D-glucose on microtubular proteins, suggesting no involvement of microfilaments in the negative effects of hyperglycemia in C1300 and
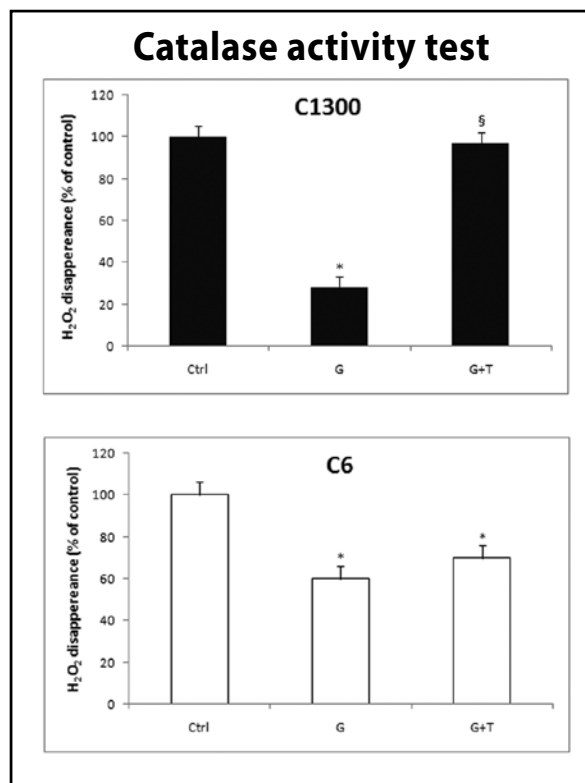
C6 cells. This could be in agreement with previous data that consider actin filaments relatively resistant to the deleterious effects of oxidative stress (Hinshaw *et al.* 1993).

The oxidative injury induced by high-D-glucose exposure through the end product 3-nitro-L-tyrosine could be related to the pattern displayed by one of the most important H_2O_2 detoxifying enzyme, catalase. The high levels of RNS overload the efficient detoxifying capability of cells leading to an inhibition of catalase antioxidant system. Our results underline strong differences between neuronal and glial cells under experimental hyperglycemic conditions. Neurons seem to be more vulnerable than astrocytes to nitric oxide and peroxynitrite-mediated damage (Bolaños *et al.* 2008). This could be due to the fact that glial cells, compared to neurons, contain a more effective antioxidant system. Indeed, we observed in D-glucose-exposed cells, a more significant reduction in catalase activity in C1300 than in C6 cells. Many authors hypothesized that the efficiency of catalase system in glial cells is improved by the cooperation with glutathione peroxidase, but this last antioxidant is

insufficient in neurons to compensate the loss of catalase activity during H_2O_2 detoxyfication. The clearance rate of peroxide decreases because of the concomitant reduction of catalase and glutathione systems, since both contribute to the detoxification from ROS. This reduced efficiency of the neuronal glutathione system might contribute to an increased nitrosative stress in neurons compared with glial cells (Makar *et al.* 1994; Bolaños *et al.* 1995; Desagher *et al.* 1996; Dringen, 2000; Dringen *et al.* 2005).

The second part of our results is related to the administration of testosterone. Interestingly, the nitrosative effects of high-glucose conditions on microtubular network displayed a noticeable weakness when the androgen was added to the cells. It is well-known that testosterone can exert biological actions on morphology, size and microtubular assembly in neuronal and glial cells (Morris *et al.* 2004). Testosterone treatment in C1300 and C6 cells leads to an increase in tubulin expression, decrease in 3-nitro-L-tyrosine amount and recovery of morphological features, growth rate, viability and catalase activity levels. The present results may confirm the neuroprotective and neurotherapeutic action of testosterone (Ahlbom *et al.* 2001; Butler *et al.* 2001; Hammond *et al.* 2001; Ramsden *et al.* 2003; Túnez *et al.* 2007; Melcangi *et al.* 2008). Thus, the positive effects that testosterone exerts against nitrosative state in C1300 and C6 cells, seem to be related to its capability to increase the activity of catalase system (Schmidt *et al.* 2005).

Interestingly, all testosterone effects were more appreciable in neuroblastoma than in glioma cell line. The differences between C1300 and C6 cells in the action of testosterone can be explained on the basis of its mechanism of action. It is well-known that testosterone exerts its biological effects through the specific intranuclear receptor. In a previous work carried out at our labs, it was demonstrated that the positive effects of testosterone on cell cultures exposed to oxidative injury were totally inhibited by the administration of the potent androgen receptor antagonist flutamide (Chisu *et al.* 2006). In the present work, a higher amount of androgen receptor was found in C1300 cells in comparison with C6. This result seems to be in agreement with those provided in the literature that reported a more predominant androgen receptor supply in neurons than in glial cells (García-Ovejero *et al.* 2002). This datum could explain the major efficiency of protective action of testosterone in neurons.

To sum up, our results underline the role played by nitrosative injuries in the consequence of hyperglycemia. Such injuries can affect the microtubular network, as the present protocol likely demonstrates. As regard the modification of proteins during hyperglycemic conditions, many data suggest that alterations of cytoskelatal network are related to two main mechanisms, i. e. glycation and oxidation (Obrosova *et al.* 2005; Sugimoto *et al.* 2008). These alterations seem to be at the basis of neurological dysfunctions, such as peripheral diabetic neuropathy and diabetic dementia, involving both neuronal and glial cells (Russell *et al.* 2008). In the last decades, some authors cast serious doubt on the role of glycation in modifying microtubular structure and function in experimental diabetes (Eaker *et al.* 1991; McLean *et al.* 1992). The present data would underline the role played by oxidative injury.

Moreover, our data seem to confirm the neuroprotective action of testosterone, indicating different effectiveness in neuronal and glial cells. This suggests possible diversified therapeutic strategies in diabetic-induced neurological alterations related to oxidative stress. In addition, a suitable model may be provided for investigating the effects of various oxidative insults on individual cell types of the CNS. Finally, it should be noted that our experimental procedures are based on cultured cells with considerable saving of laboratory animal lives.

REFERENCES

1 Aebi H (1984). Catalase in vitro. Methods Enzymol. **105**: 121–126.
2 Acarin L, Peluffo H, Barbeito L, Castellano B, Gonzalez B (2005). Astroglial nitration after postnatal excitotoxic damage: correlation with nitric oxide sources, cytoskeletal, apoptotic and antioxidant proteins. J Neurotrauma. **22**: 189–200.
3 Ahlbom E, Prins GS, Ceccatelli S (2001). Testosterone protects cerebellar granule cells from oxidative stress-induced cell death through a receptor mediated mechanism. Brain Res. **892**: 255–262.
4 Allen DA, Yaqoob MM, Harwood SM (2005). Mechanisms of high glucose-induced apoptosis and its relationship to diabetic complications. J Nutr Biochem. **16**: 705–713.
5 Andersen JK (2004). Oxidative stress in neurodegeneration: cause or consequence? Nat Med. **10**: 18–25.
6 Blanchard-Fillion B, Prou D, Polydoro M., Spielberg D, Tsika E, Wang Z, et al. (2006). Metabolism of 3-nitrotyrosine induces apoptotic death in dopaminergic cells. J. Neurosci. **26**: 6124–6130.
7 Bolaños JP, Delgado-Esteban M, Herrero-Mendez A, Fernandez-Fernandez S, Almeida A (2008). Regulation of glycolysis and pentose-phosphate pathway by nitric oxide: impact on neuronal survival. Biochim Biophys Acta. **1777**: 789–793.
8 Bolaños JP, Heales SJ, Land JM, Clark JB (1995). Effect of peroxynitrite on the mitochondrial respiratory chain: differential susceptibility of neurones and astrocytes in primary culture. J Neurochem. **64**: 1965–1972.
9 Butler R, Leigh PN, Gallo JM (2001). Androgen-induced up-regulation of tubulin isoforms in neuroblastoma cells. J Neurochem. **78**: 854–861.
10 Chance B, Sies H, Boveris A (1979). Hydroperoxide metabolism in mammalian organs. Physiol Rev. **59**: 527–605.
11 Chang W, Webster DR, Salam AA, Gruber D, Prasad A, Eiserich JP, et al. (2002). Alteration of the C-terminal amino acid of tubulin specifically inhibits myogenic differentiation. J Biol Chem. **277**: 30690–30698.
12 Cheng C, Zochodne DW (2003). Sensory neurons with activated caspase-3 survive long-term experimental diabetes. Diabetes. **52**: 2363–2371.
13 Chisu V, Manca P, Lepore G, Gadau S, Zedda M, Farina V (2006). Testosterone induces neuroprotection from oxidative stress. Effects on catalase activity and 3-nitro-L-tyrosine incorporation into alpha-tubulin in a mouse neuroblastoma cell line. Arch Ital Biol. **144**: 63–73.

14 Coers S, Tanzer L, Jones KJ (2002). Testosterone treatment attenuates the effects of facial nerve transection on glial fibrillary acidic protein (GFAP) levels in the hamster facial motor nucleus. Metab Brain Dis. **17**: 55–63.

15 Delaney CL, Russell JW, Cheng HL, Feldman EL (2001). Insulin-like growth factor-I and over-expression of Bcl-xL prevent glucose-mediated apoptosis in Schwann cells. J Neuropathol Exp Neurol. **60**: 147–160.

16 Desagher S, Glowinski J, Premont J (1996). Astrocytes protect neurons from hydrogen peroxide toxicity. J Neurosci. **16**: 2553–2562.

17 Drel VR, Pacher P, Stevens MJ, Obrosova IG (2006). Aldose reductase inhibition counteracts nitrosative stress and poly(ADP-ribose) polymerase activation in diabetic rat kidney and high-glucose-exposed human mesangial cells. Free Radic Biol Med. **40**: 1454–1465.

18 Dringen R (2000). Metabolism and functions of glutathione in brain. Prog Neurobiol. **62**: 649–671.

19 Dringen R, Pawlowski PG, Hirrlinger J (2005). Peroxide detoxification by brain cells. J Neurosci Res. **79**: 157–165.

20 Eaker EY, Angelastro JM, Purich DL, Sninsky CA (1991). Evidence against impaired brain microtubule protein polymerization at high glucose concentrations or during diabetes mellitus. J Neurochem. **56**: 2087–2093.

21 Eiserich JP, Estevez AG, Bamberg TV, Ye YZ, Chumley PH, Beckman JS, et al. (1999). Microtubule dysfunction by posttranslational nitrotyrosination of alpha-tubulin: a nitric oxide-dependent mechanism of cellular injury. Proc Natl Acad Sci USA. **96**: 6365–6370.

22 Emerit J, Edeas M, Bricaire F (2004). Neurodegenerative diseases and oxidative stress. Biom Pharm. **58**: 39–46.

23 Erck C, Peris L, Andrieux A, Meissirel C, Gruber AD, Vernet M, et al. (2005). A vital role of tubulin-tyrosine-ligase for neuronal organization. Proc Natl Acad Sci USA. **102**: 7853–7858.

24 Fukushima N, Furuta D, Hidaka Y, Moriyama R, Tsujiuchi T (2009). Post-translational modifications of tubulin in the nervous system. J Neurochem. 109: 683–693.

25 Gadau S, Lepore G, Zedda M, Manca P, Chisu V, Farina V (2008). D-glucose induces microtubular changes in C1300 neuroblastoma cell line through the incorporation of 3-nitro-L-tyrosine into tubulin. Arch Ital Biol. **146**: 107–117.

26 García-Ovejero D, Veiga S, García-Segura LM, Doncarlos LL (2002). Glial expression of estrogen and androgen receptors after rat brain injury. J Comp Neurol. **450**: 256–271.

27 Guillod-Maximin E, Lorsignol A, Alquier T, Pénicaud L (2004). Acute intracarotid glucose injection towards the brain induces specific c-fos activation in hypothalamic nuclei: involvement of astrocytes in cerebral glucose-sensing in rats. J Neuroendocrinol. **16**: 464–471.

28 Halliwell B (2006). Oxidative stress and neurodegeneration: where are we now? J Histochem. **97**: 1634–1658.

29 Halliwell B (1992). Reactive oxygen species and the central nervous system. J Neurochem. **59**: 1609–1623.

30 Halliwell B (2001). Role of free radicals in the neurodegenerative diseases: therapeutic implications for antioxidant treatment. Drugs Aging. **18**: 685–716.

31 Hammond J, Le Q, Goodyer C, Gelfand M, Trifiro M, LeBlanc A (2001). Testosterone-mediated neuroprotection through the androgen receptor in human primary neurons. J Neurochem. **77**: 1319–1326.

32 Hertz L, Kala G (2007). Energy metabolism in brain cells: effects of elevated ammonia concentrations. Metab Brain Dis. **22**: 199–218.

33 Hinshaw DB, Miller MT, Omann GM Beals TF, Hyslop PA (1993). A cellular model of oxidant-mediated neuronal injury. Brain Res. **615**: 13–26.

34 Hollensworth SB, Shen CC, Sim JE, Spitz DR, Wilson GL, LeDoux SP (2000). Glial cell specific responses to menadione-induced oxidative stress. Free Rad Biol Med. **28**: 1161–1174.

35 Khanna P, Nehru B (2007). Antioxidant enzymatic system in neuronal and glial cells enriched fractions of rat brain after aluminum exposure. Cell Mol Neurobiol. **27**: 959–969.

36 Kurosinski P, Gotz J (2002). Glial cells under physiologic and pathologic conditions. Arch Neurol. **59**: 1524–1528.

37 Makar TK, Nedergaard M, Preuss A, Gelbard AS, Perumal AS, Cooper AJ (1994). Vitamin E, ascorbate, glutathione, glutathione disulfide, and enzymes of glutathione metabolism in cultures of chick astrocytes and neurons: evidence that astrocytes play an important role in antioxidative processes in the brain. J Neurochem. **62**: 45–53.

38 Marcos S, Moreau J, Backer S, Job D, Andrieux A, Bloch-Gallego E (2009). Tubulin tyrosination is required for the proper organization and pathfinding of the growth cone. PLoS One. **4**: 5405.

39 Maritim AC, Sanders RA, Watkins JB (2003). Diabetes, oxidative stress and antioxidants: a review. J Biochem Mol Toxicol. **17**: 24–38.

40 McCall AL (2004). Cerebral glucose metabolism in diabetes mellitus. Eur J Pharmacol. **490**: 147–158.

41 McLean WG, Pekiner C, Cullum NA, Casson IF (1992). Posttranslational modifications of nerve cytoskeletal proteins in experimental diabetes. Mol Neurobiol. **6**: 225–237.

42 Melcangi RC, Garcia-Segura LM, Mensah-Nyagan AG (2008). Neuroactive steroids: state of the art and new perspectives. Cell Mol Life Sci. **65**: 777–797.

43 Mihm MJ, Schanbacher BL, Wallace BL, Wallace LJ, Uretsky, NJ, Bauer JA (2001). Free 3-nitrotyrosine causes striatal neurodegeneration in vivo. J Neurosci. **21**: 1–5.

44 Morris JA, Jordan CL, Breedlove SM (2004). Sexual differentiation of the vertebrate nervous system. Nat Neurosci. **7**: 1034–1039.

45 Obrosova IG, Mabley JG, Zsengellér Z, Charniauskaya T, Abatan OI, Groves JT et al. (2005). Role for nitrosative stress in diabetic neuropathy: evidence from studies with a peroxynitrite decomposition catalyst. FASEB J. **19**: 401–403.

46 Pacher P, Obrosova IG, Mabley JG, Szabó C (2005). Role of nitrosative stress and peroxynitrite in the pathogenesis of diabetic complications. Emerging new therapeutical strategies. Curr Med Chem. **12**: 267–275.

47 Peluffo H, Shacka JJ, Ricart K, Bisig CG, Martinez-Palma L, Pritsch O et al. (2004). Induction of motor neuron apoptosis by free 3-nitro-L-tyrosine. J Neurochem. **89**: 602–612.

48 Phung, AD, Soucek, K, Kubala, L, Harper, RW, Chloe Bulinski, J, Eiserich, JP (2006). Posttranslational nitrotyrosination of alpha-tubulin induces cell cycle arrest and inhibits proliferation of vascular smooth muscle cells. Eur J Cell Biol. **85**: 1241–1252.

49 Pike CJ (2001). Testosterone attenuates beta-amyloid toxicity in cultured hippocampal neurons. Brain Res. **919**: 160–165.

50 Ramsden M, Shin TM, Pike CJ (2003). Androgens modulate neuronal vulnerability to kainate lesion. Neuroscience. **122**: 573–578.

51 Russell JW, Berent-Spillson A, Vincent AM, Freimann CL, Sullivan KA, Feldman EL (2008). Oxidative injury and neuropathy in diabetes and impaired glucose tolerance. Neurobiol Dis. **30**: 420–429.

52 Sayre LM, Perry G, Smith MA (2008). Oxidative stress and neurotoxicity. Chem Res Toxicol. **21**: 172–188.

53 Schmidt AJ, Krieg JC, Vedder H (2005). Effects of steroid hormones on catalase activity in neuronal and glial cell systems. Eur Neuropsychopharmacol. **15**: 177–183.

54 Sugimoto K, Yasujima M, Yagihashi S (2008). Role of advanced glycation end products in diabetic neuropathy. Curr Pharm Des. **14**: 953–961.

55 Tanzer L, Jones KJ (2004). Neurotherapeutic action of testosterone on hamster facial nerve regeneration: temporal window of effects. Horm Behav. **45**: 339–344.

56 Túnez I, Feijóo M, Collado JA, Medina FJ, Peña J, Muñoz Mdel C, et al. (2007). Effect of testosterone on oxidative stress and cell damage induced by 3-nitropropionic acid in striatum of ovariectomized rats. Life Sci. **80**: 1221–1227.

57 Thuraisingham RC, Nott CA, Dodd SM, Yaqoob MM (2000). Increased nitrotyrosine staining in kidneys from patients with diabetic nephropathy. Kidney Int. **57**: 1968–1972.

58 Zedda M, Lepore G, Gadau S, Manca P, Farina V (2004). Morphological and functional changes induced by the amino acid analogue 3-nitrotyrosine in mouse neuroblastoma and rat glioma cell lines. Neurosci Lett. **363**: 190–193.

59 Zhou FQ, Cohan CS (2004). How actin filaments and microtubules steer growth cones to their targets. J Neurobiol. **58**: 84–91.